

# ServeGen: Workload Characterization and Generation of Large Language Model Serving in Production

Yuxing Xiang<sup>1,2</sup> Xue Li<sup>2</sup> Kun Qian<sup>2</sup>  
Wenyuan Yu<sup>2</sup> Ennan Zhai<sup>2</sup> Xin Jin<sup>1</sup>

<sup>1</sup>*School of Computer Science, Peking University* <sup>2</sup>*Alibaba Group*

<https://arxiv.org/abs/2505.09999>

Presenter: Zijian Dai

# Contents

1

Background

---

2

Characterizing Language Workloads

---

3

Characterizing Multimodal Workloads

---

4

Characterizing Reasoning Workloads

---

5

Workload Generation

---

6

Discussion

---

1

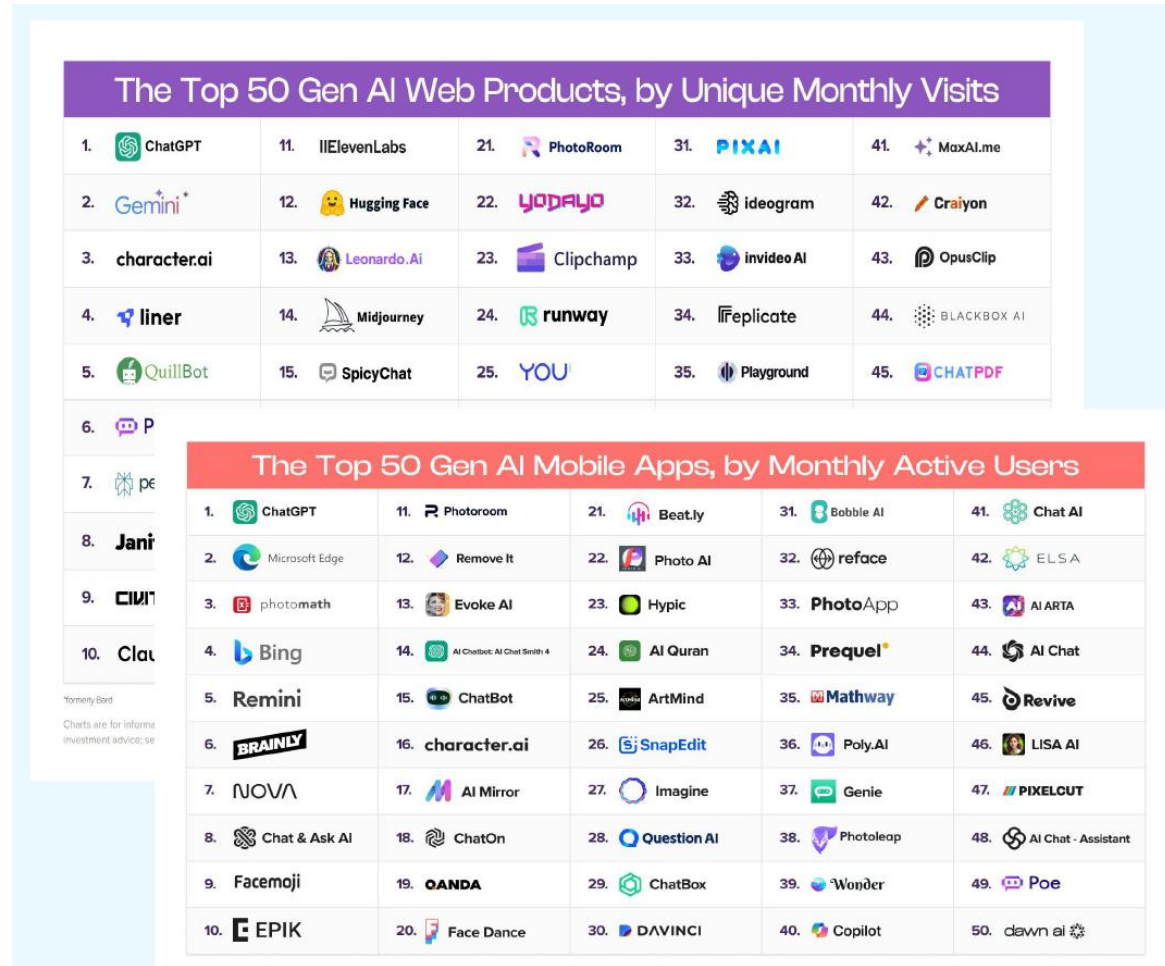
# Background

---



# Background

- The increasingly application of large models is driving a growing demand for inference services.



- Inference engines are constantly evolving.

vLLM

NVIDIA TensorRT-LLM

🤗 Transformers

SGL

高吞吐

最好兼容性

LLM++

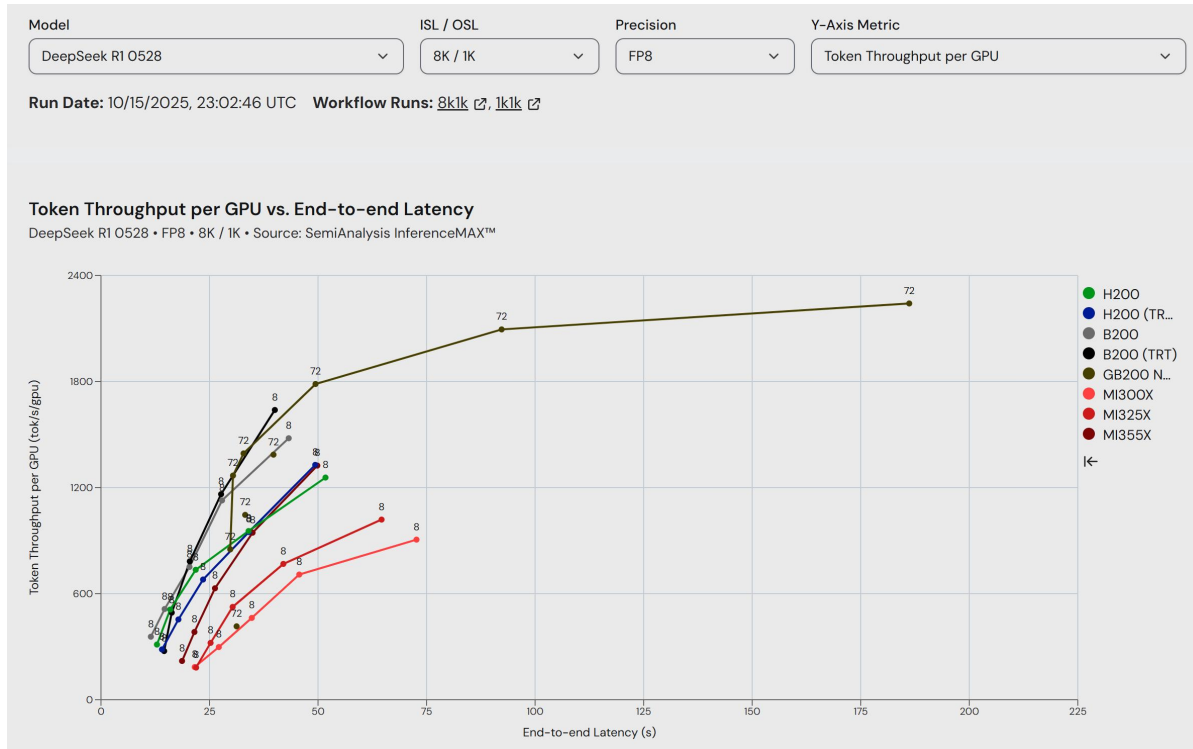
OpenVINO™

MLX

工作在端侧

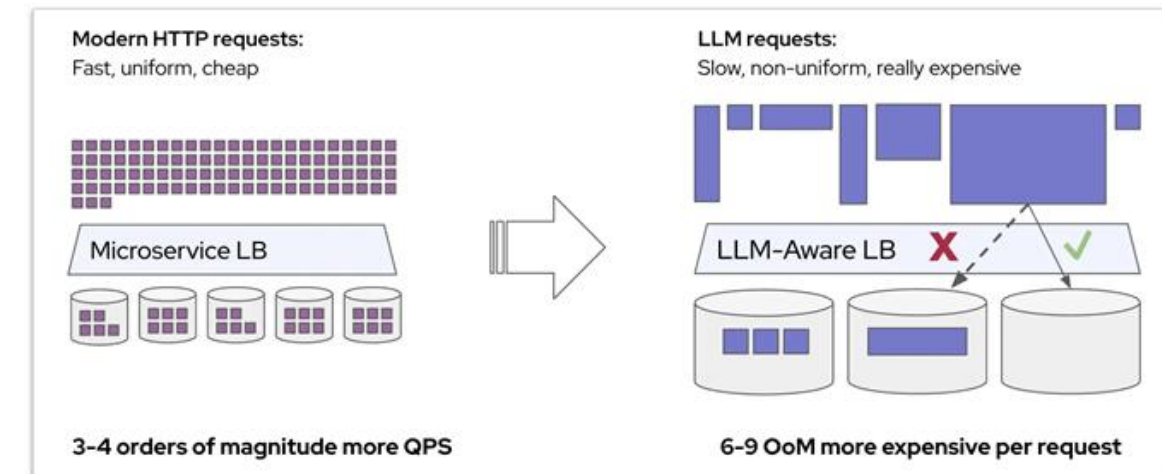
# Background

- Benchmarking is critical for motivating LLM serving techniques and systems



<https://inferenceMAX.semianalysis.com/>

- Existing understanding of real-world LLM serving workloads is limited due to the lack of a comprehensive workload characterization.



- Many studies use **Naïve** approach to generate workloads, For request Inter-arrival time:
  1. Sampled from Poisson or Gamma Processes
  2. Scaled from published traces with datasets
- Analysis and experiments on real-world workload show that benchmarks based on these **Naïve** methods are inaccurate, leading to 50% under-provisioning in instance provisioning.

# Open source workload of LLM serving

## ● Qwen-Bailian Anonymous Dataset

*Scenarios: ChatGPT-like service, task automation with API calling*

```
{  
    "chat_id": 159,  
    "parent_chat_id": 55,  
    "timestamp": 61.114,  
    "input_length": 521,  
    "output_length": 132,  
    "type": "text",  
    "turn": 2,  
    "hash_ids": [1089, 1090, 1091, 6326, ..., 13148]  
}
```

## ● Mooncake

*Scenarios: conversation, tool&agent , synthetic*

Listing 2: Request samples.

```
{  
    "timestamp": 27000,  
    "input_length": 6955,  
    "output_length": 52,  
    "hash_ids": [46, 47, 48, 49, 50, 51, 52,  
                53, 54, 55, 56, 57, 2111, 2112]  
}  
{  
    "timestamp": 30000,  
    "input_length": 6472,  
    "output_length": 26,  
    "hash_ids": [46, 47, 48, 49, 50, 51, 52,  
                53, 54, 55, 56, 57, 2124]  
}
```

1. <https://github.com/alibaba-edu/qwen-bailian-usagetraces-anon>  
Optimizing KVCache cache design.  
(KVCache@ATC'25)

2. <https://github.com/kvcache-ai/Mooncake/tree/main/FAST25-release/traces>  
(Mooncake@FAST'25)

## ● BurstGPT

*Scenarios: Azure Openai Conversation*

1	Timestamp	Model	Request tokens	Response tokens	Total tokens	Log Type
2	5	ChatGPT	472	18	490	Conversation log
3	45	ChatGPT	1087	230	1317	Conversation log
4	118	GPT-4	417	276	693	Conversation log
5	185	ChatGPT	1360	647	2007	Conversation log
6	214	ChatGPT	185	215	400	Conversation log
7	233	GPT-4	586	293	879	Conversation log
8	261	ChatGPT	37	1656	1693	Conversation log
9	267	ChatGPT	54	503	557	Conversation log
10	410	ChatGPT	1528	414	1942	Conversation log
11	535	ChatGPT	89	370	459	Conversation log
12	560	GPT-4	549	362	911	Conversation log
13	638	ChatGPT	172	69	241	Conversation log
14	686	GPT-4	969	206	1175	Conversation log
15	741	ChatGPT	97	137	234	Conversation log
16	771	GPT-4	1574	501	2075	Conversation log
17	821	ChatGPT	253	239	492	Conversation log
18	966	ChatGPT	23	344	367	Conversation log
19	974	ChatGPT	509	207	716	Conversation log
20	1028	ChatGPT	387	349	736	Conversation log
21	1072	ChatGPT	733	180	913	Conversation log
22	1106	ChatGPT	0	0	0	Conversation log
23	1129	ChatGPT	1305	477	1782	Conversation log
24	1278	ChatGPT	17	382	399	Conversation log
25	1449	ChatGPT	601	557	1158	Conversation log

3. <https://github.com/HPMLL/BurstGPT/tree/main>  
in  
(BurstGPT)

2

# Characterizing Language Workloads



# Workload source: Alibaba Bailian Platform

**Duration:** from January to April 2025

**Models:** 12

**Requests:** 3.54B

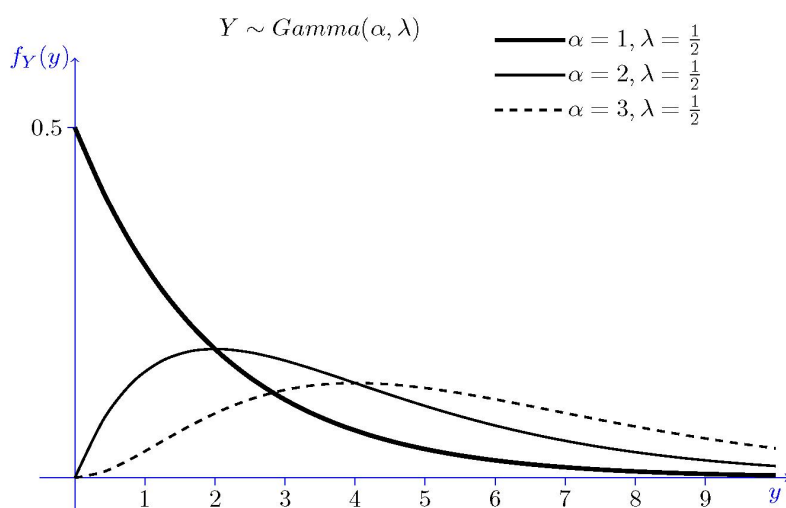
**GPUs:** 10K distributed in dozens of regions and zones

**Table 1.** The list of workloads and models in our study.

Category	Name	Model	Description	Workload Information
Language	M-large	Qwen-Max	Largest, general-purpose	February
	M-mid	Qwen-Plus	Balanced, general-purpose	February
	M-small	Qwen-Turbo	Cheapest, general-purpose	February
	M-long	Qwen-Long with a 10M context length	Long-document comprehension	January (one week)
	M-rp	Tongyi-Xingchen	Role-playing	January (one week)
	M-code	Tongyi-Lingma	Code completion	January (one week)
Multimodal	mm-image	Qwen2.5-VL-72B	Image & text input	March
	mm-audio	Qwen2-Audio-7B	Audio & text input	March
	mm-video	Qwen2.5-VL-72B	Video & text input	March
	mm-omni	Qwen2.5-Omni-7B	Omni-modal input	April (one week)
Reasoning	deepseek-r1	DeepSeek-R1-671B	Full reasoning model	March (one week)
	deepqwen-r1	DeepSeek-R1-distill-Qwen-32B	Distilled reasoning model	March (one week)

## 随机过程相关知识

时间间隔的随机分布：(Exponential / Gamma / Weibull)



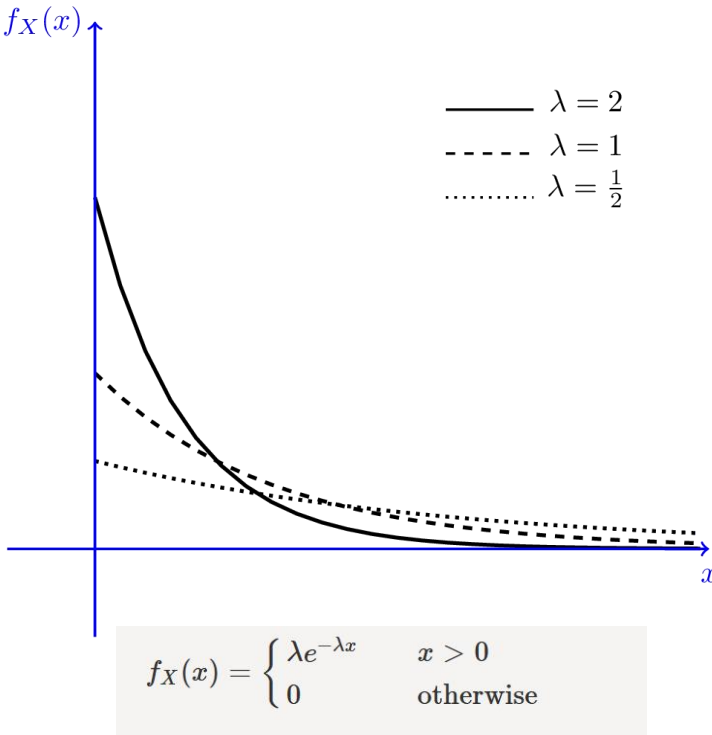
$$f_X(x) = \begin{cases} \frac{\lambda^\alpha x^{\alpha-1} e^{-\lambda x}}{\Gamma(\alpha)} & x > 0 \\ 0 & \text{otherwise} \end{cases}$$

## gamma分布

$\alpha$ 是事件发生的次数

例如：商店第 $\alpha$ 个顾客到来、第 $\alpha$ 个热线电话呼入、第 $\alpha$ 个人口出生的时间间隔

$\alpha = 1$  时退化 



$$f_X(x) = \begin{cases} \lambda e^{-\lambda x} & x > 0 \\ 0 & \text{otherwise} \end{cases}$$

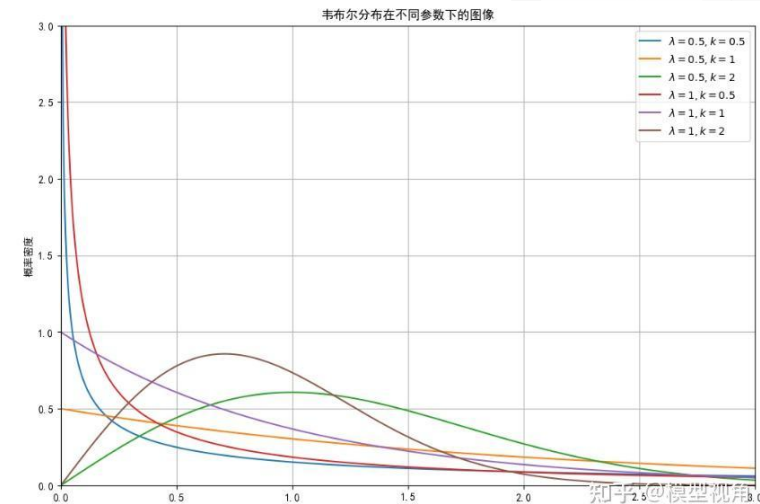
# Exponential 分布

例如：商店下1个顾客到来、下1个热线电话呼入、下1个人口出生的时间间隔

均值  $\mu = 1/\lambda$

标准差  $\sigma = \frac{1}{\lambda}$

变异系数  $CV = \frac{\sigma}{\mu} = 1$



$$f(t) = k\lambda t^{k-1} e^{-\lambda t^k} \quad \text{for } t \geq 0$$

# Weibull分布

例如：机器损坏时间

$\leftarrow k=1$  时退化

# Request Arrival Pattern

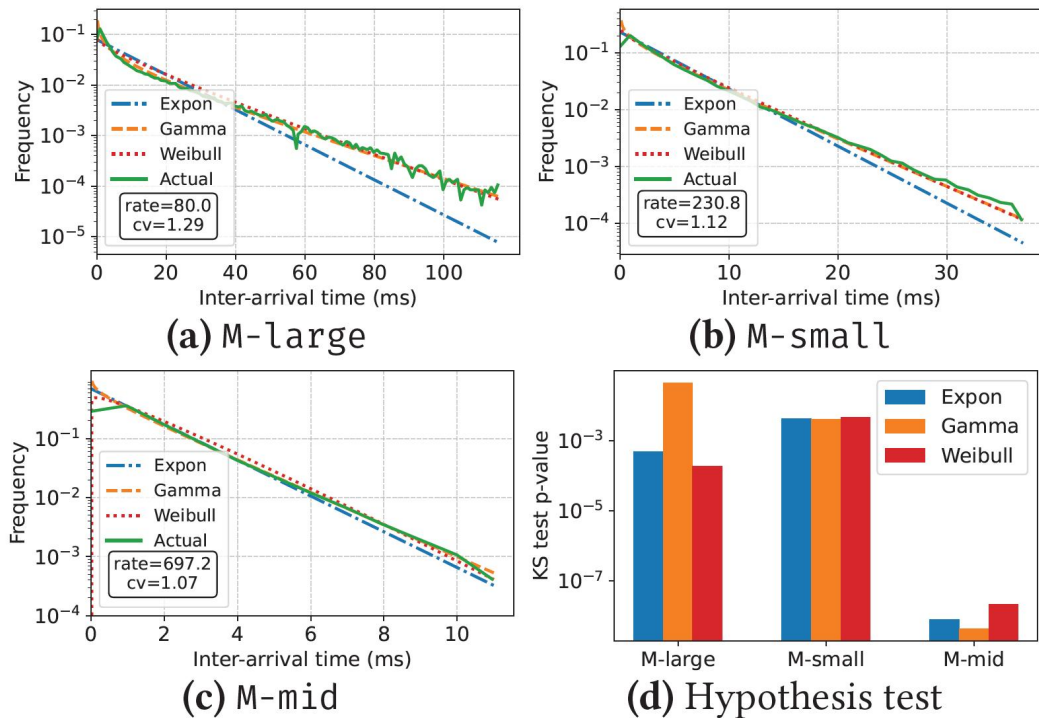


Figure 1. Inter-arrival time characterization.

**Finding 1:** The short-term arrival of LLM requests is often **bursty ( $CV > 1$ )**, exhibiting complex patterns beyond any single stochastic process.

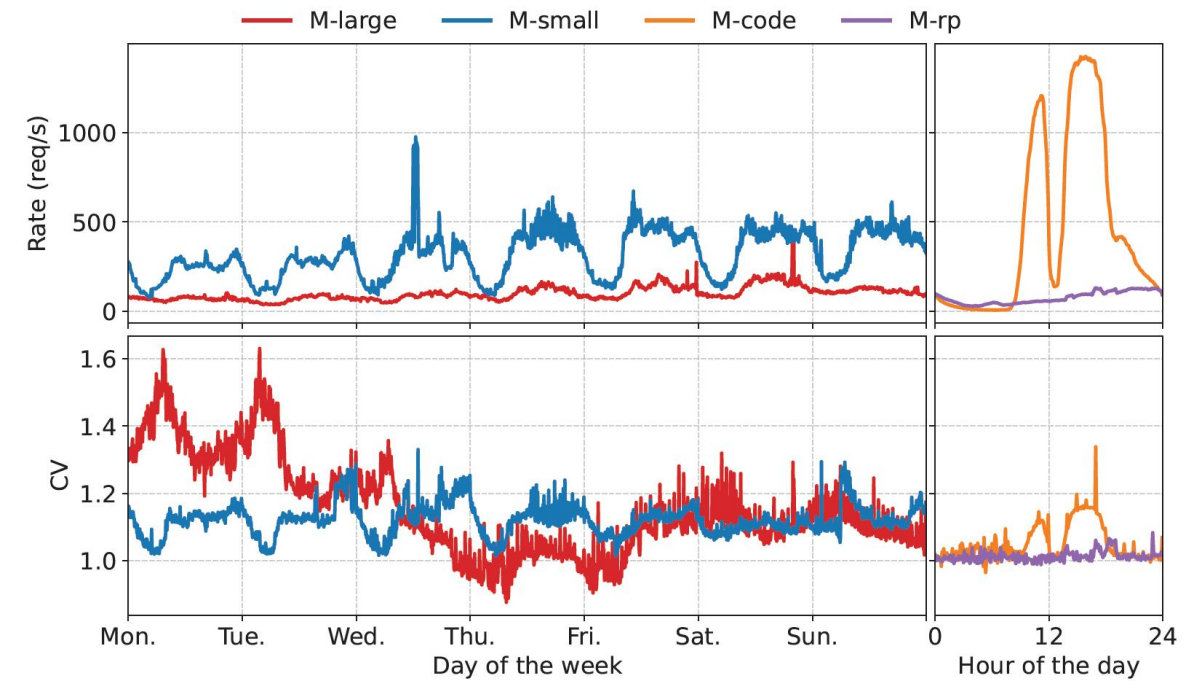
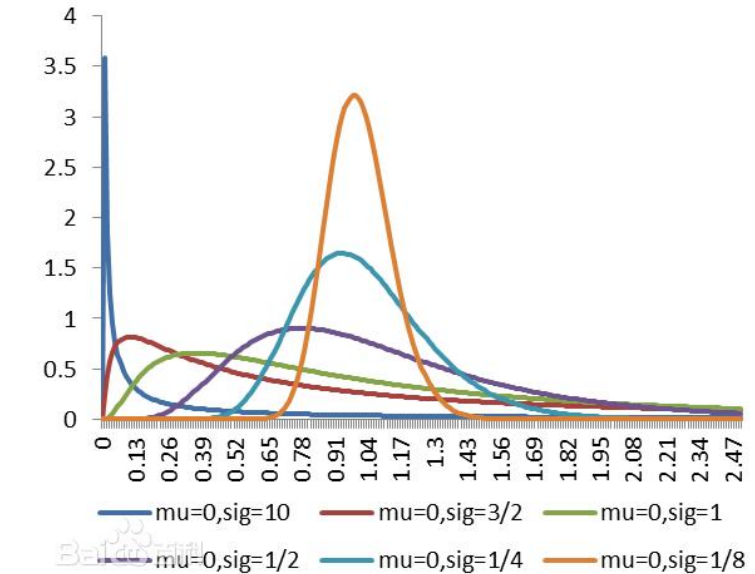
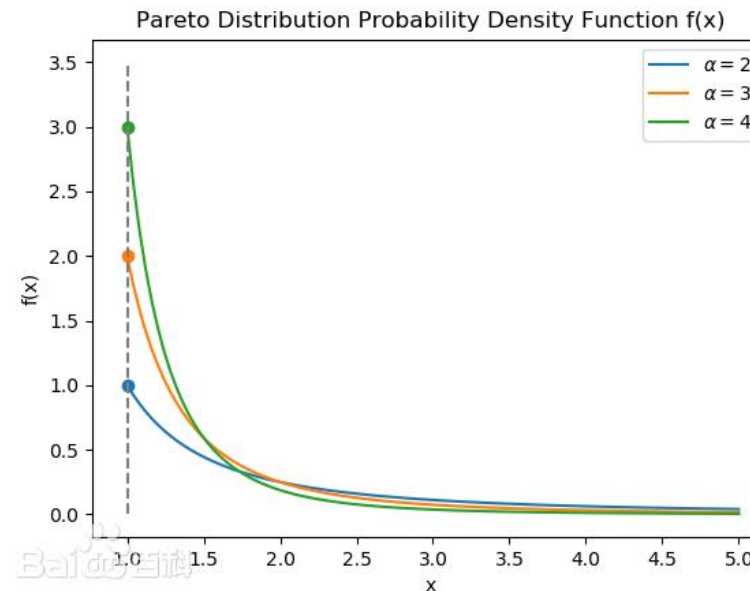
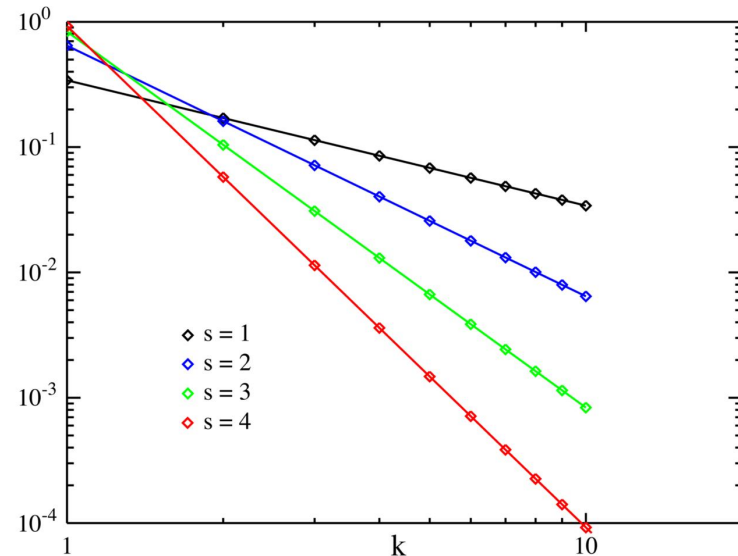


Figure 2. Long-term rate and CV shifts.

**Finding 2:** The arrival of LLM serving requests shows a diverse shifting pattern in terms of rate and burstiness, calling for adaptive system design.

# 随机过程相关知识

请求prompt长度的随机分布：(Pareto/Log-normal/zipf)



$$p(x) = \begin{cases} 0, & \text{if } x < x_{\min}; \\ \frac{k x_{\min}^k}{x^{k+1}}, & \text{if } x > x_{\min}. \end{cases}$$

## Zipf分布

例如：语料库里，一个单词出现的频率与它在频率表里的排名成反比

## Pareto分布

例如：财富在个人之间的分布（即20%的人拥有80%的财富）

$$f(x, \mu, \sigma) = \begin{cases} \frac{1}{x \sqrt{2\pi}\sigma} \exp\left[-\frac{1}{2\sigma^2}(\ln x - \mu)^2\right], & x > 0 \\ 0, & x \leq 0 \end{cases}$$

## Log-normal分布

例如：收入、人口的分布

# Input and Output Length Distribution

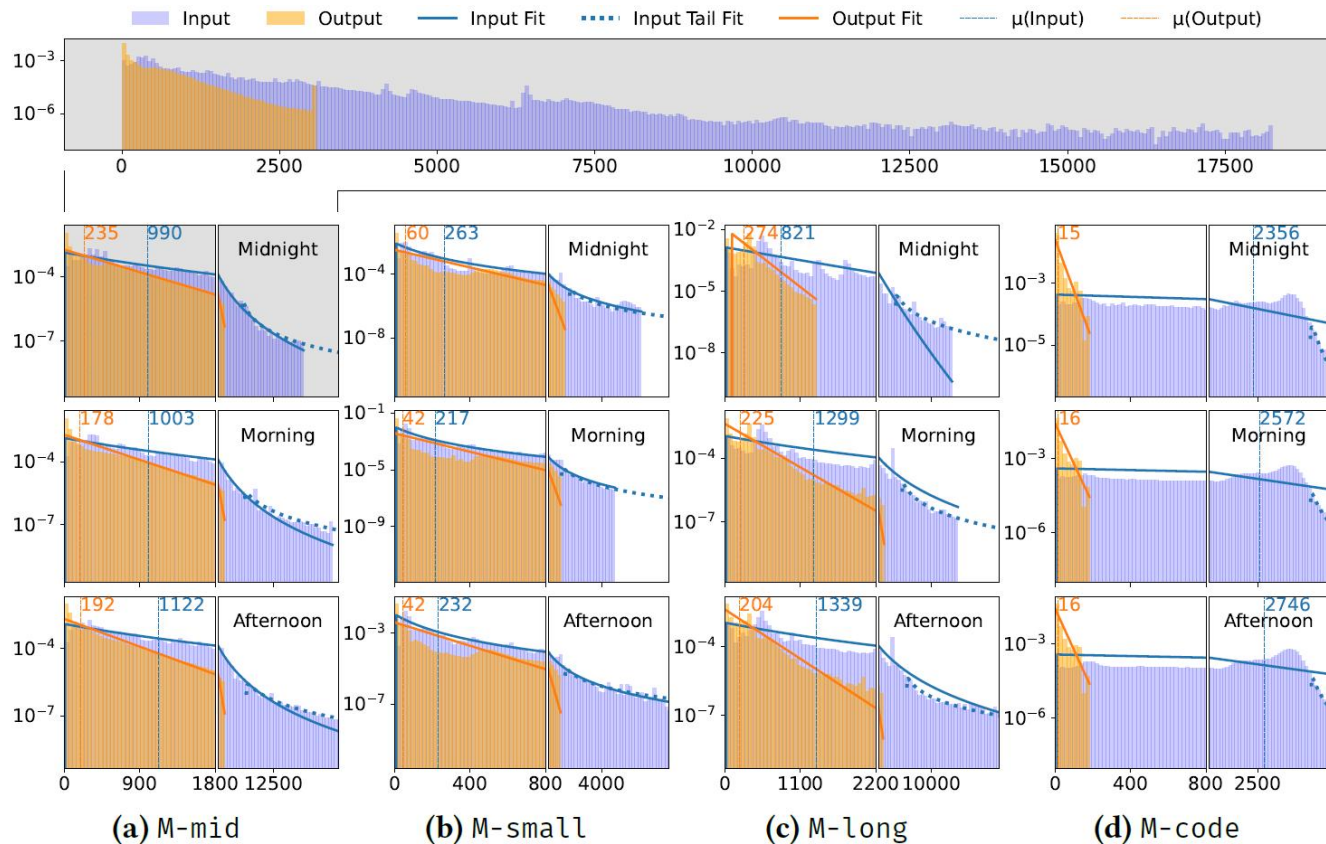


**Figure 3.** Input and output length distribution. *x-axis*: # tokens; *y-axis*: frequency. Each subfigure corresponds to a specific workload and time period, split to two consecutive x-scales to better visualize the shift in average lengths (left) as well as the tail distribution (right).

**Finding 3:** The input length distribution can be modeled with a mixture of Pareto and Log-normal distributions, and the output with Exponential distributions.

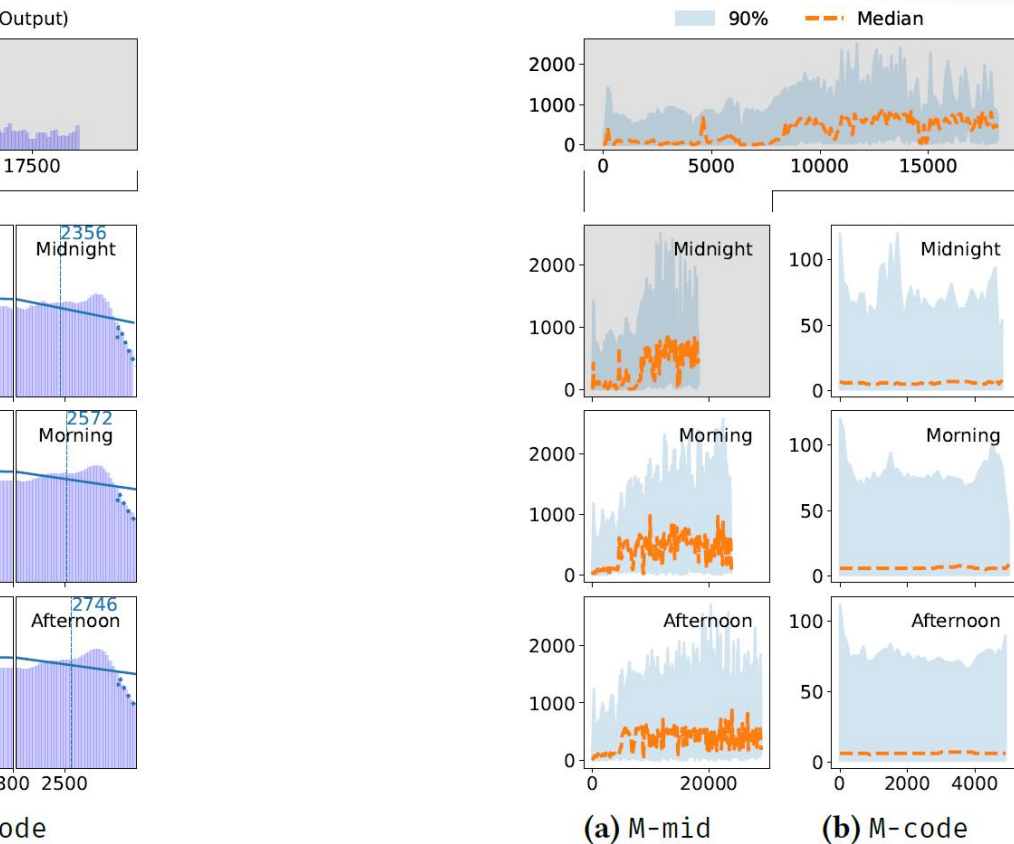


**Figure 4.** Input and output length correlation. *x-axis*: input length; *y-axis*: output length.

# Client Decomposition

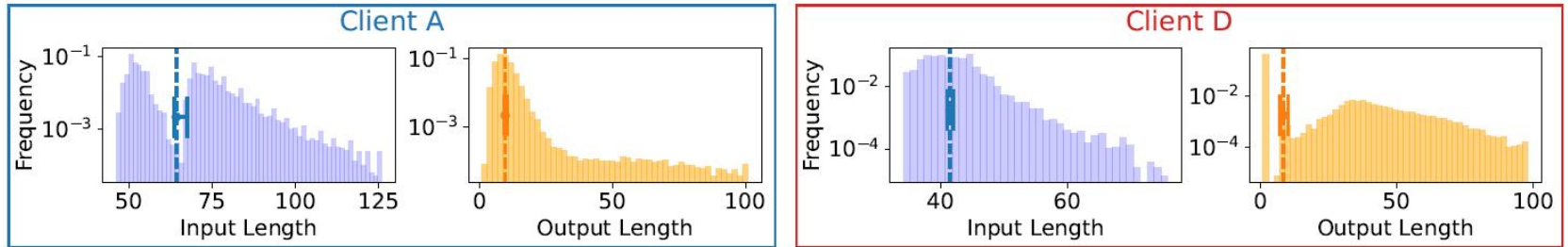
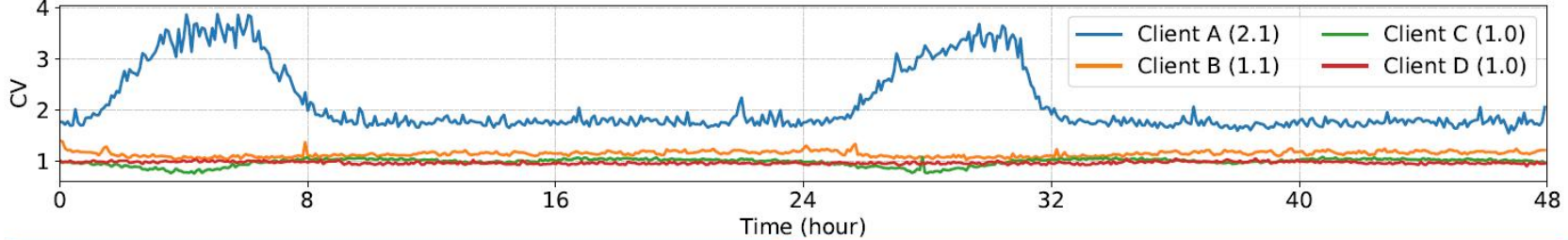
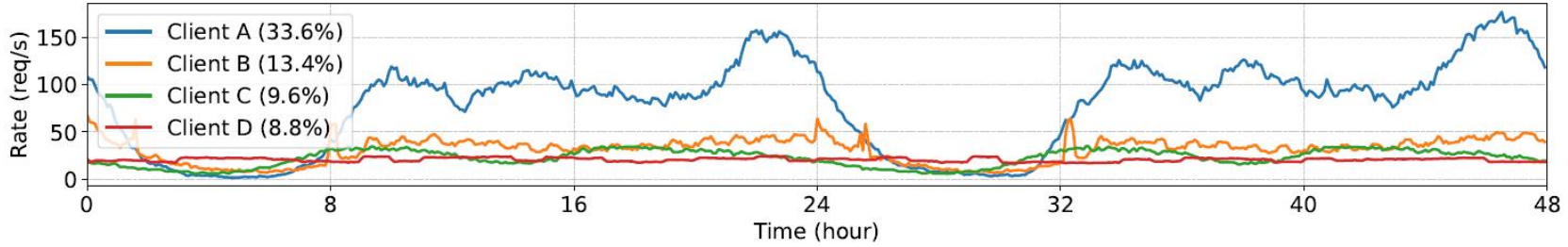
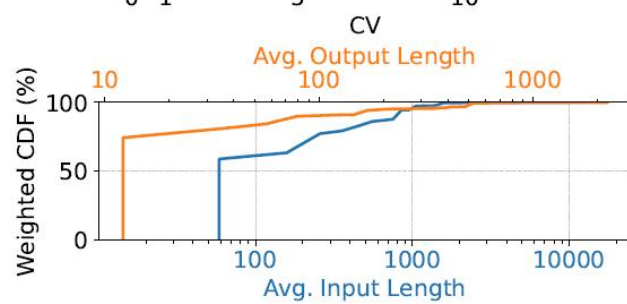
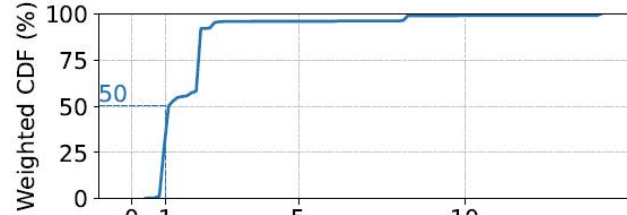
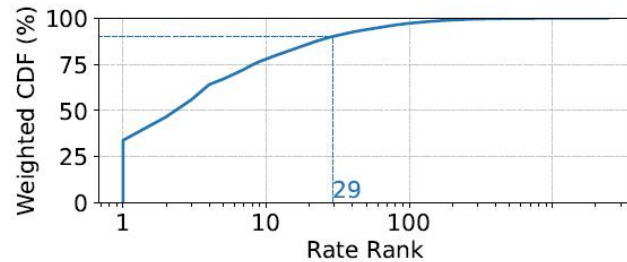


**Figure 5.** Client heterogeneity in terms of rate, etc. All CDFs are weighted by client rates.

**Figure 6.** Characterization of the top four clients in the M-small workload in isolation, using the first 48-hour data from Figure 2. Vertical lines in the last-row subfigures indicate average input/output lengths, and error bars show the range of average lengths in 1-hour windows.

observed 2,412 clients in 48-hour

**Finding 5:** Real-world workloads consist of heterogeneous clients with skewed arrival rates. The top clients and their rate fluctuations largely explain the shifting workload patterns.

# 3

# Characterizing Multimodal Workloads



# Modality Load Variance

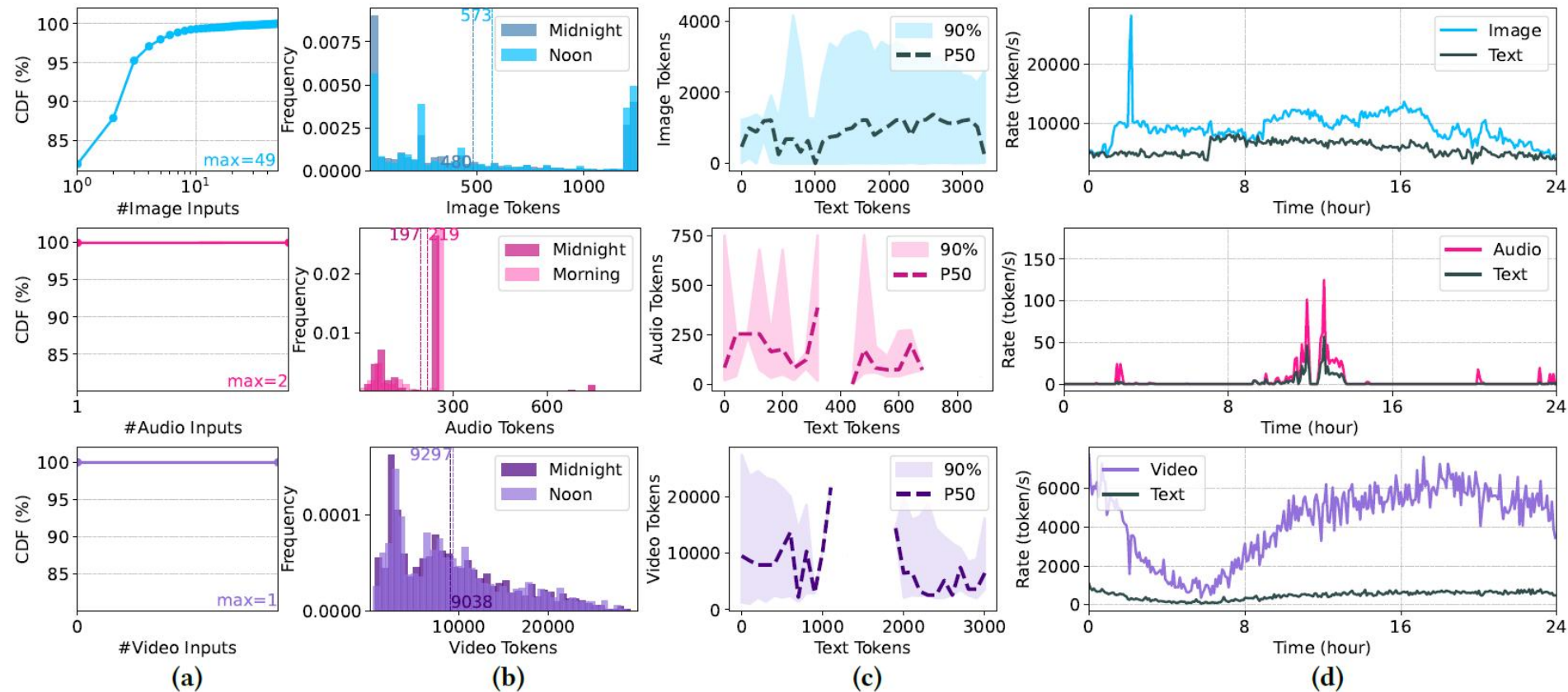


**Figure 7.** Characterization of multimodal inputs in three different workloads. *Rows*: mm-image, mm-audio, and mm-video, respectively. *Columns*: (a) number of multimodal inputs per request; (b) tokenized length distribution of multimodal inputs; (c) correlation between text tokens and multimodal tokens; (d) overall arrival rate of multimodal and text tokens.

- multimodal inputs are more likely to have standard sizes (depending on upstream applications)
- correlation between text tokens and multimodal tokens is weak

# Modality Load Variance

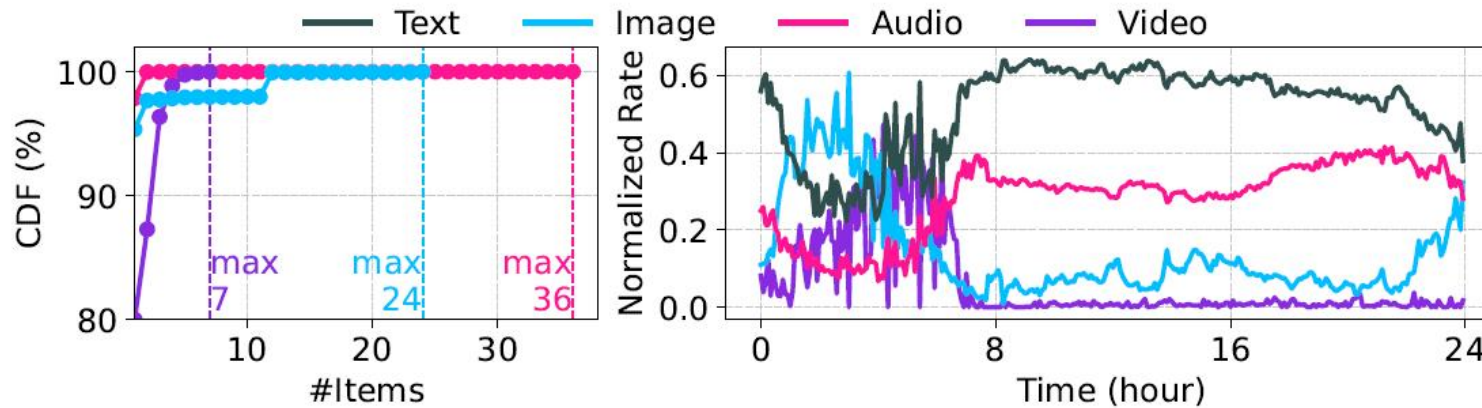


**Figure 8.** Characterization of omni-modal inputs in mm-omni. *Left:* number of multimodal inputs per request. *Right:* arrival rate of multimodal and text tokens, normalized by the total input rate.

- omni-modality workload exhibits more complex variability

**Finding 6:** Multimodal data distributions exhibit irregular and independent shifts, underscoring significant load variance across modalities.

# Modality Load Variance

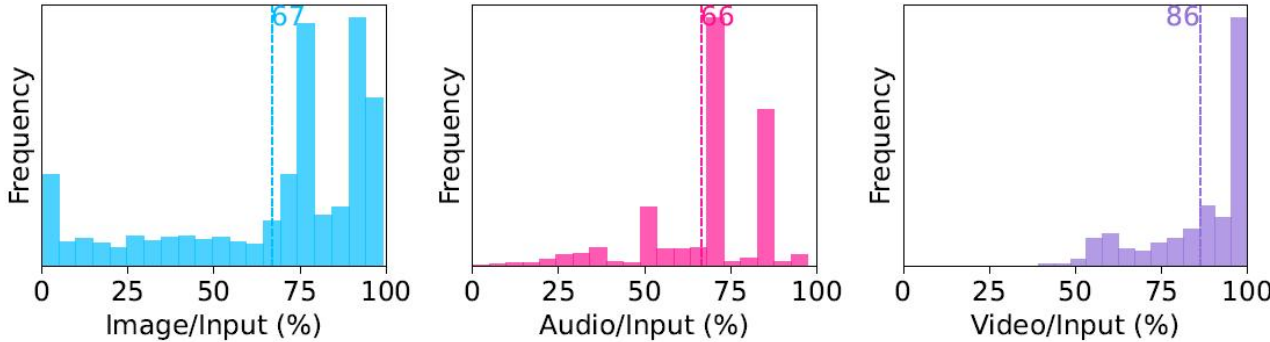
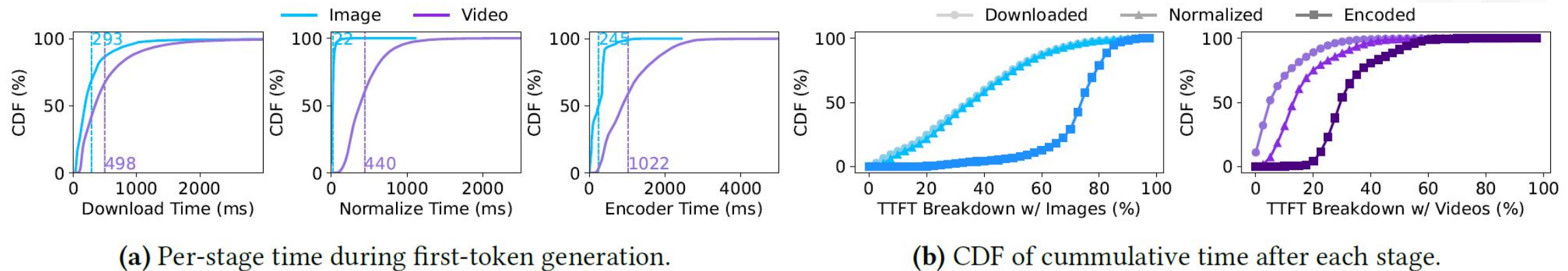


**Figure 9.** Ratio of multimodal input tokens per request in mm-image, mm-audio, and mm-video. Numbers indicate the average ratio.

- real multimodal requests are heterogeneous

**Finding 7:** Multimodal requests are heterogeneous with diverse ratios of multimodal inputs per request

# Request Heterogeneity



(a) Per-stage time during first-token generation.

(b) CDF of cumulative time after each stage.

**Figure 10.** Breakdown of first-token time when serving requests with image or video inputs (mm-image and mm-video).

Finding 8:

the download, normalization, and encoding stages for tokenizing multimodal inputs all contribute to considerable extra overhead,

which leads to prolonged TTFTs that necessitate tailored optimizations.

# Request Heterogeneity

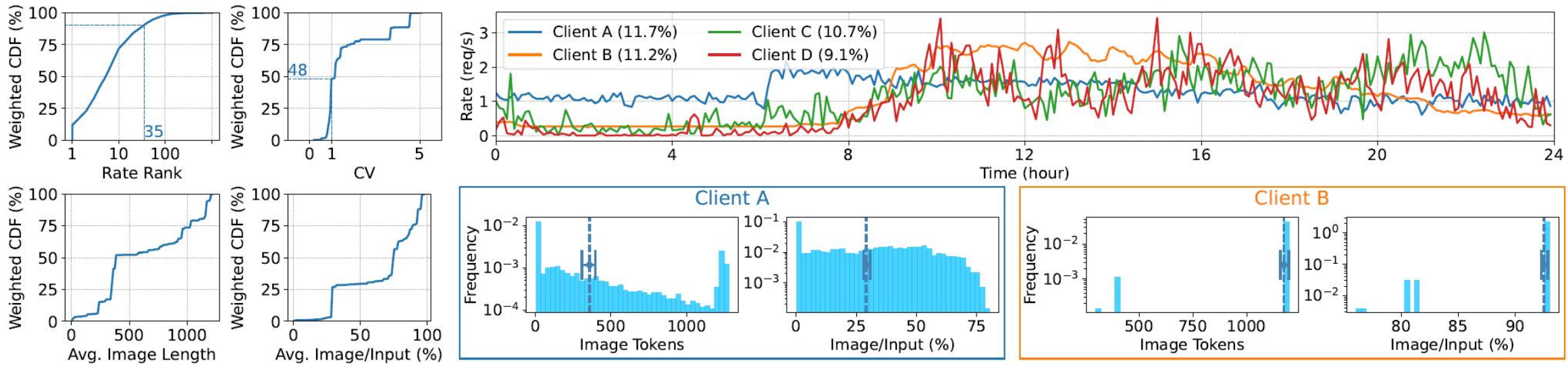


Figure 11. Client characterization for mm-image. CDFs are weighted by rates.

Among 1,036 multimodal clients

Figure 12. Behavior of top clients in mm-image in isolation. Vertical lines in the last-row subfigures indicate average lengths, and error bars show the range of average lengths within a day.

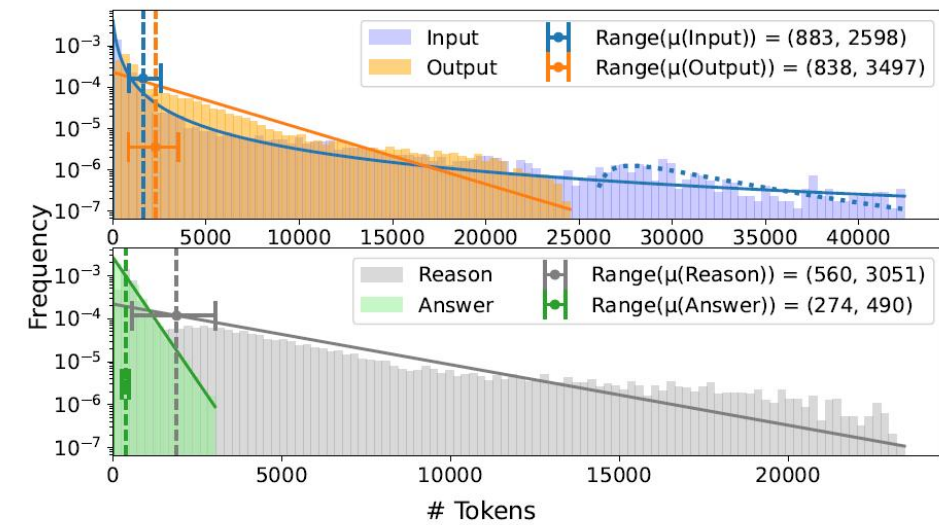
**Finding 8:** Top clients in multimodal workloads exhibit diverse behaviors, and characterizing them helps explain the overall workload patterns.

# 4

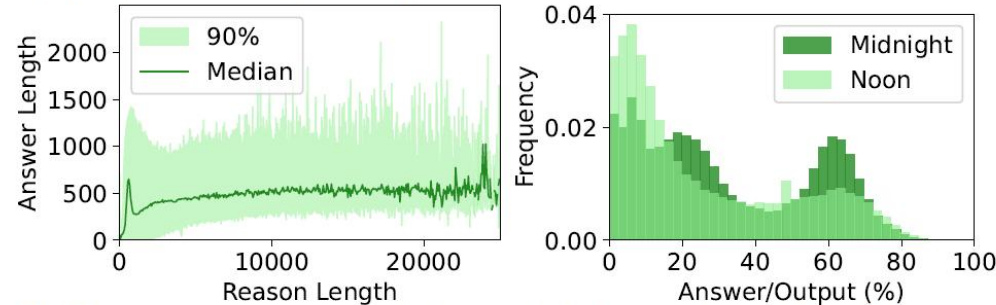
## Characterizing Reasoning Workloads



# Characterizing Reasoning Workloads



(a) Input and output length distribution, in one-hour windows.

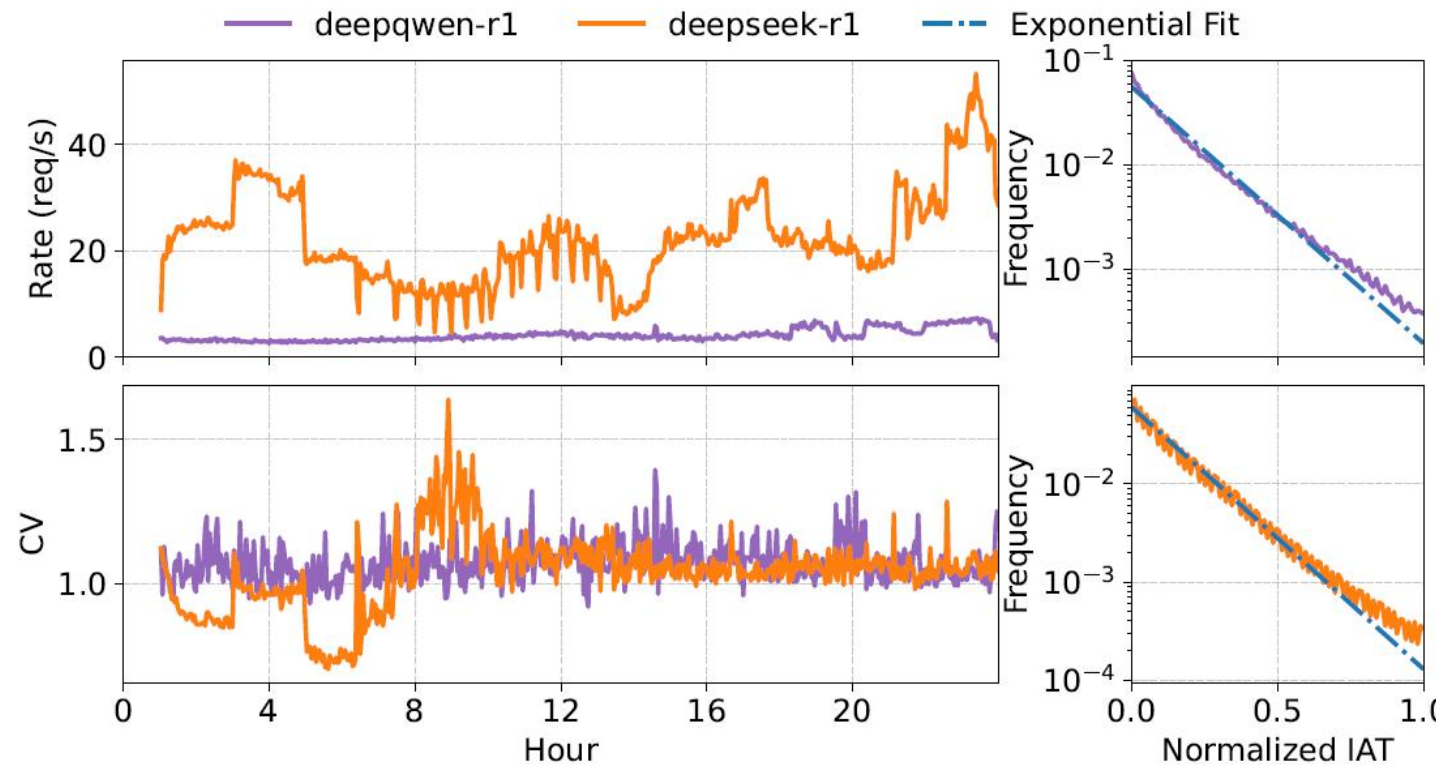


(b) Reason-answer correlation. (c) Output length breakdown.

**Figure 13.** Characterization of input and output lengths for the deepseek-r1 workload in one day. Error bars in (a) indicate the range of average lengths over the day.

**Finding 9:** Reasoning workloads exhibit longer and more variable output lengths, due to the reason tokens. In relation, reason and answer lengths display stronger positive correlation, as well as a unique bimodal ratio.

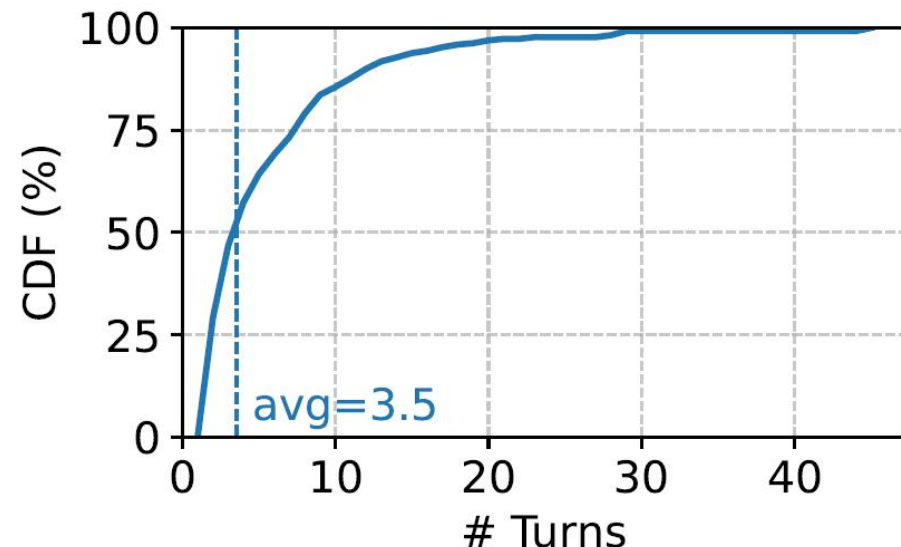
# Characterizing Reasoning Workloads



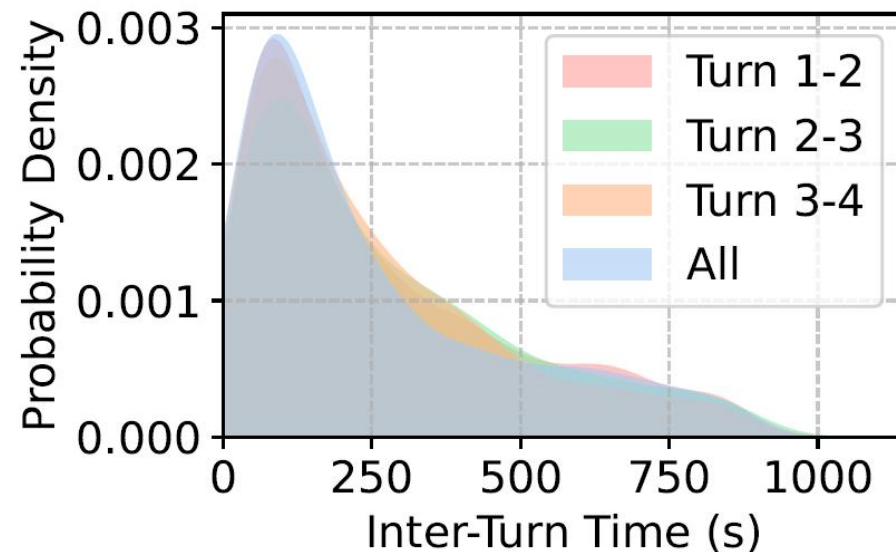
- Exponential distribution
- Less bursty arrivals (compared with Non-reasoning model in Figure 2)

**Figure 14.** Characterization of request arrival patterns in deepseek-r1 and deepqwen-r1. *Left:* Rate and burstiness shifts over a day. *Right:* Normalized inter-arrival time distributions.

## Characterizing multi-turn conversations



(a) CDF of conversation lengths.



(b) PDF of inter-turn times.

**Figure 15.** Characterization of conversations in deepseek-r1.

- average conversation lengths = 3.5
- Similar distribution of inter-turn time

# Characterizing Reasoning Workloads

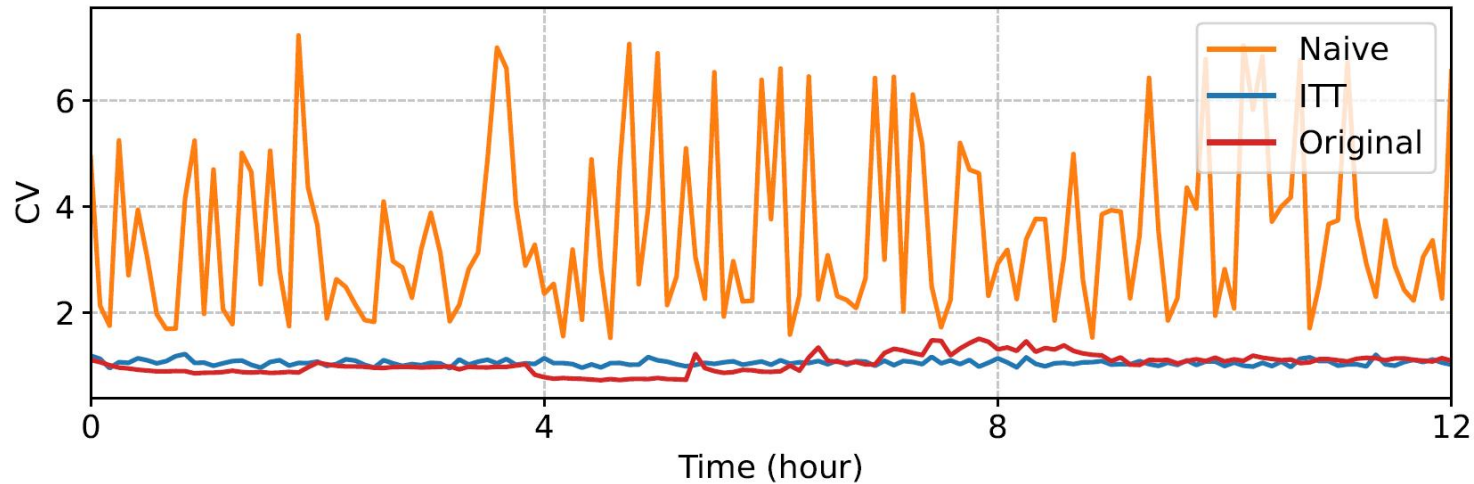


**Figure 16.** Comparison of two upsampling methods for a workload containing only multi-turn requests.

multi-turn requests constitute almost 10% of the deepseek-r1 workload

Use two upsampling methods (scale from multi-turn requests workload to original workload)

**Naive**: agnostic about the conversations (Figure 15b), scales the inter-arrival time

**ITT**: scaling the arrival time between conversations, leaving the ITT distribution unchanged

**Finding 10:** Request arrival in reasoning workloads is impacted by the reoccurring pattern of multi-turn conversations and appears less bursty.

# Characterizing Reasoning Workloads

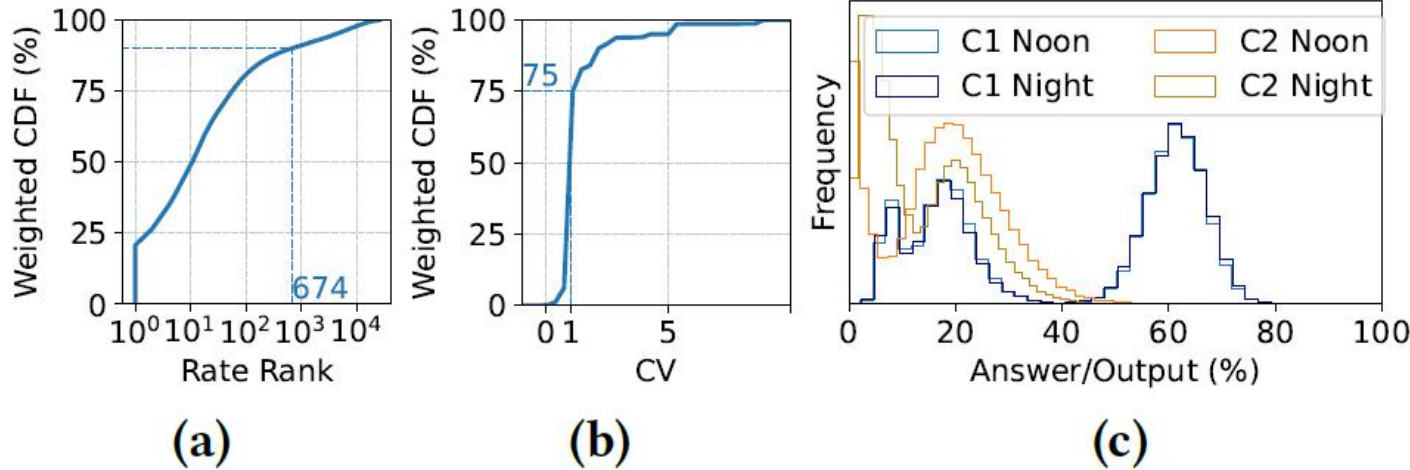


**Figure 17.** Client decomposition for deepseek-r1. (a) weighted CDF of client arrival rate. (b) weighted CDF of client burstiness. (c) output length breakdown of top clients (C1 and C2).

Among 25,913 clients

**Finding 11 :** Clients in reasoning workloads exhibit less skewed rates and less bursty arrivals, while also showing the bimodal pattern in terms of data distributions.

- Top clients in deepseek-r1 are shown to be less substantial
- The proportion of non-bursty clients is also significantly higher
- Bimodal distribution in the breakdown of request output lengths

# 5

# Workload Generation



# Workload Generation: ServeGen Framework

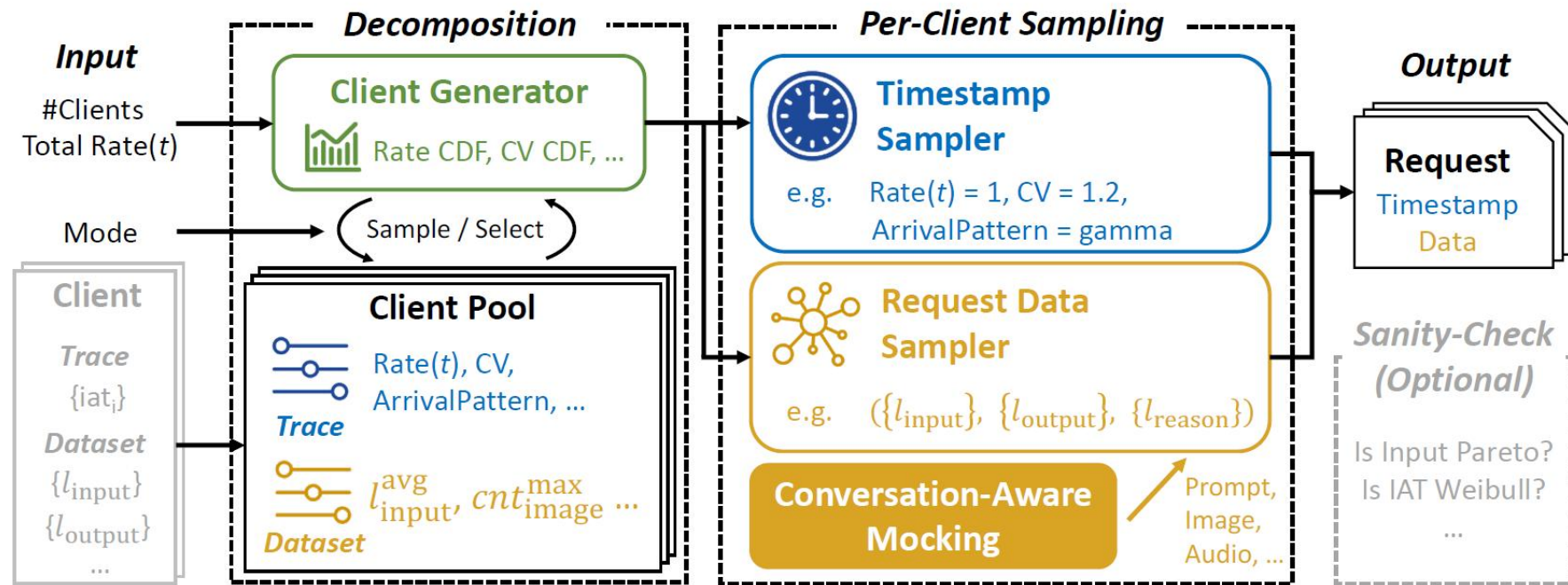


**Figure 18.** Overview of the ServeGen framework. The color gray indicates optional requirements; e.g., users can still use ServeGen without providing additional client information.

<https://github.com/alibaba/ServeGen>

# Workload Generation: ServeGen Framework

# deepseek-r1 72 clients

```
1   {
2     "0": {
3       "input_tokens": "{45: 0.009666283084004603, 46: 0.011737629459148446, 47: 0.00391254315",
4       "output_tokens": "{64: 0.00023014959723820482, 77: 0.00023014959723820482, 82: 0.00046",
5       "reason_ratio": "{0.0: 0.0, 0.001996007984031936: 0.0, 0.003992015968063872: 0.0, 0.005",
6     },
7     "21600": {
8       "input_tokens": "{17: 0.001718213058419244, 45: 0.005154639175257732, 46: 0.01202749146",
9       "output_tokens": "{122: 0.001718213058419244, 130: 0.001718213058419244, 191: 0.0017182",
10      "reason_ratio": "{0.0: 0.0, 0.001996007984031936: 0.0, 0.003992015968063872: 0.0, 0.005",
11    },
12    "43200": {
13      "input_tokens": "{}",
14      "output_tokens": "{}",
15      "reason_ratio": "{}"
16    },
17    "64800": {
18      "input_tokens": "{}",
19      "output_tokens": "{}",
20      "reason_ratio": "{}"
21  }
22 }
```

## Request length distribution

1	0	0	0		0	0
2	600	0	0		0	0
3	1200	0	0		0	0
4	1800	0	0		0	0
5	2400	0.085	6.69324386291654	Gamma	0.02232167101916883	73.01783087211976
6	3000	0.39	0.9137465123848778	Gamma	1.1977013397371243	2.074553310327594
7	3600	0.4216666666666667	1.0022801337212446	Gamma	0.9954552823877275	2.385870887198335
8	4200	0.4333333333333335	0.9140982433836469	Gamma	1.1967798028260763	1.911871171139863
9	4800	0.3366666666666667	1.0008881807649188	Gamma	0.9982260023520739	2.31995639433158
10	5400	0	0		0	0
11	6000	0	0		0	0
12	6600	0	0		0	0
13	7200	0	0		0	0
14	7800	0.3533333333333333	1.9996034406619674	Gamma	0.25009916934658716	11.012446779262042
15	8400	0.3083333333333335	1.152778512053871	Gamma	0.752503033285289	4.2769508383437875
16	9000	0.3266666666666666	0.8970360969242444	Weibull	1.1167491378227001	3.1569971349039734
17	9600	0.3333333333333333	1.0543935635041897	Gamma	0.8994862062683567	3.331600442916639

# Request Arrival Pattern

`chunk-O-trace.csv`

<https://github.com/alibaba/ServeGen>

# Comparison of workload generation accuracy

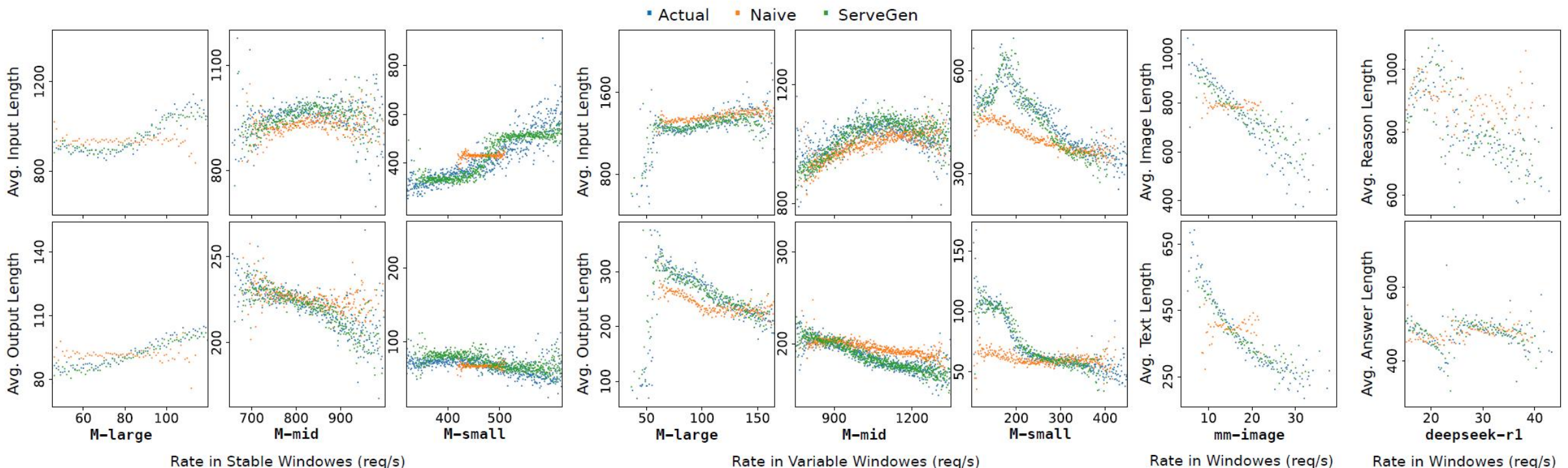
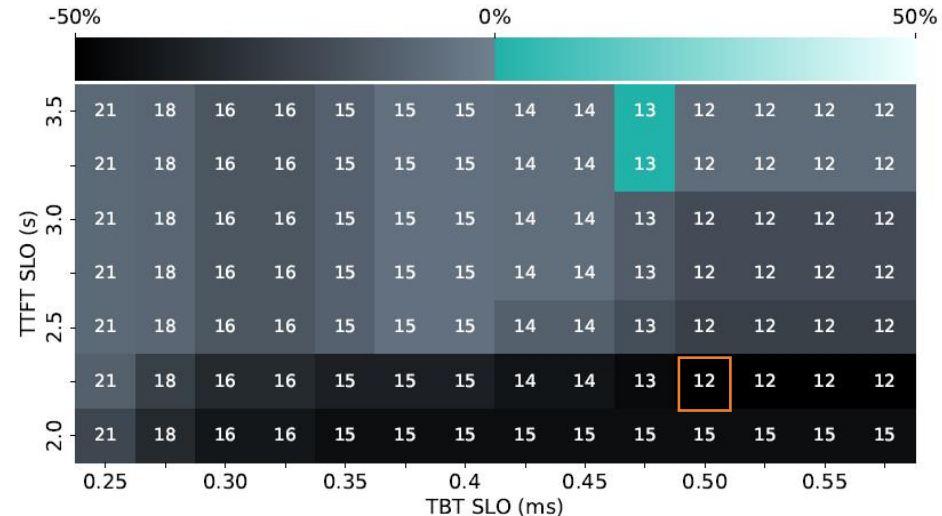


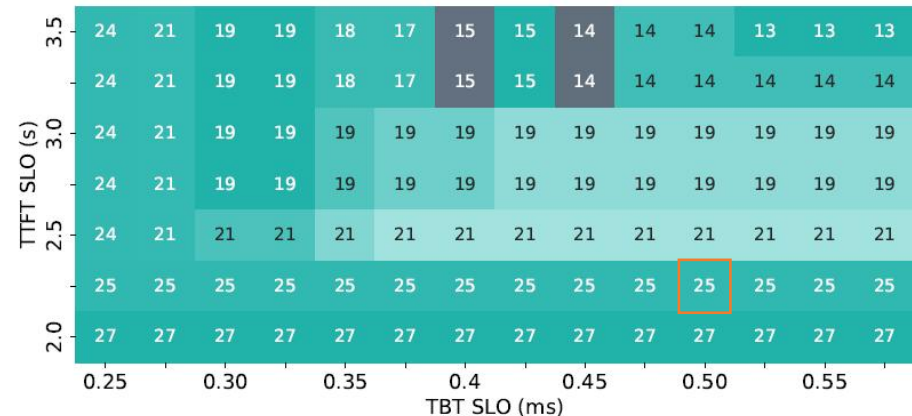
**Figure 19.** Comparison of workload generation accuracy.

- ServeGen matches the actual plot much better
- Naïve barely capture the correlation between rates and data distributions  
(large or small short-term rates are likely caused by bursty top clients, and the workload data distributions are expected to shift correspondingly toward or away from the client data distributions.)

# UseCase: Instance Provisioning



(a) Provisioning with NAIVE.



(b) Provisioning with ServeGen.

**Figure 20.** Provisioning results using the NAIVE approach and ServeGen. In each cell, the number indicates the provisioned instances, while the color shows the over-provisioning percentage.

- Workload:

10-minute period of M-large comprising 30,000 requests (generated by NAÏVE and Servegen approach)

- Each Instance:

2 \* NVIDIA A100 (80GB) GPUs  
vLLM(Pipeline parallelism) + Qwen2.5-14B model

- Method:

benchmark one instance using both NAÏVE and Servegen approach, determine the maximum rate that meets SLO targets (P99), and derive the required instance count

- Results:

TTFT 2.25s TBT 0.5s

ServeGen: 25 instances (4% over the actual)

Naïve: 12 instances (50% under-provisioning)

6

# Discussion



## Key takeaway

1. Real-world LLM Serving Workload request arrivals exhibit a complex bursty pattern that goes beyond any single stochastic process
2. Most nondeterministic patterns in request arrivals (e.g., bursts) and length distributions (e.g., high dynamics over time) are caused by **several top clients**, while the behaviors of most clients remain stable and predictable
3. Multi-turn conversations have Similar distribution of inter-turn time
4. A significant portion of TTFT stems from preprocessing (i.e., downloading, normalization, and encoding). highlights the importance of conducting full-stack optimizations

## Discussion

**1. LLM serving with plugin calls/function call (i.e., web searches, database queries, or calling external APIs):**

For future work

**2. prefix KV cache:**

Not investigated, due to user privacy considerations.

**3. Generalization:**

Could record customize workload and reproduce.

☰

# Thank you !

## 13. Workload Generation: ServeGen Framework

	ServeGen	Naive
<b>Sampling method</b>	Resamples based on <b>client decomposition</b>	Resamples the <b>entire workload as a whole</b> , ignoring individual clients.
<b>Realism of generated workload</b>	Produces more <b>realistic</b> workloads — scatter plots closely match actual workload.	Workload diverges from real patterns in both rate and data distribution.
<b>Variability (request rate)</b>	Accurately reflects real variability — includes wide horizontal spread in scatter plots.	Often <b>less variable</b> in stable periods despite global burstiness.
<b>Rate–data correlation</b>	Captures correlation between <b>request rate and data distribution</b> , as real top clients cause correlated bursts.	Fails to capture such correlation — rate and data distribution are independent.